

High-order Dy multipole motifs observed in DyB₂C₂ with resonant soft x-ray Bragg diffraction

A.M. Mulders¹, U. Staub¹, V. Scagnoli¹, S.W. Lovesey^{2,5}, E. Balcar³,
T. Nakamura⁴, A. Kikkawa⁵, G. van der Laan⁶ and J.M. Tonnerre⁷

¹*Paul Scherrer Institut, CH 5232 Villigen PSI, Switzerland*

²*ISIS, Rutherford Appleton Laboratory, Chilton, Oxfordshire OX11 0QX, United Kingdom*

³*Vienna University of Technology, Atominstut, Stadionallee 2. A1020, Vienna, Austria*

⁴*SPRING-8/JASRI, Mikazuki, Sayo, Hyogo 679-5198, Japan*

⁵*RIKEN Harima Institute, Mikazuki, Sayo, Hyogo 679-5148, Japan*

⁶*Daresbury Laboratory, Warrington, Cheshire WA4 4AD, UK and*

⁷*CNRS Grenoble, 38042 Grenoble Cedex 9, France*

(Dated: March 23, 2022)

Resonant soft x-ray Bragg diffraction at the Dy $M_{4,5}$ edges has been exploited to study Dy multipole motifs in DyB₂C₂. Our results are explained introducing the intra-atomic quadrupolar interaction between the core $3d$ and valence $4f$ shell. This allows us to determine for the first time higher order multipole moments of dysprosium $4f$ electrons and to draw their precise charge density. The Dy hexadecapole and hexacontatetrapole moment have been estimated at -20% and $+30\%$ of the quadrupolar moment, respectively. No evidence for the lock-in of the orbitals at T_N has been observed, in contrast to earlier suggestions. The multipolar interaction and the structural transition cooperate along c but they compete in the basal plane explaining the canted structure along $[110]$.

PACS numbers: 71.70.Ch; 75.40.Cx; 78.70.Ck

Resonant x-ray Bragg scattering (RXS) has recently become a powerful tool in modern solid state physics to investigate magnetic, orbital and charge order phenomena associated with electronic degrees of freedom. Especially in transition metal oxides, and, possibly, actinide compounds, various phenomena can occur simultaneously and it is not easy to identify the exact role and interplay of the various order parameters. However, in rare earth based compounds, orbital and magnetic order occur more autonomously from the lattice as the $4f$ electrons are shielded by the outer $5d$ electrons. Electronic orbital motifs are usually labeled antiferroquadrupolar (AFQ) or ferroquadrupolar (FQ) but higher order multipoles are not established by observations. Argon atoms in an excited state with $l=3$ show a significant presence of the higher order multipole moments as concluded from electron scattering [1], but in the solid state multipoles beyond rank 4 have never been detected. Yet the alignment of higher multipoles to the surrounding charge in the lattice is likely. For $4f$ electrons ($l=3$) multipoles up to rank 6 are present and this results in a undulated and aspheric charge density. Which multipoles dominate these orbital order transitions remains a rather controversial topic as exemplified in CeB₆ [2], NpO₂ [3] and URu₂Si₂ [4]. Using soft x-ray resonant Bragg scattering (SXRS), we have obtained the first direct evidence of high-order Dy multipole moment motifs in DyB₂C₂.

DyB₂C₂ has attracted much attention lately as its high AFQ ordering temperature $T_Q=24.7$ K allows to study this phenomenon conveniently. At room temperature, DyB₂C₂ crystallizes in the tetragonal $P4/mbm$ structure and undergoes a structural transition with small alternating shifts of B and C atoms along c at T_Q

[5] which reduces the symmetry to $P4_2/mnm$ [6]. Below $T_N=15.3$ K antiferromagnetic order (AFM) is observed with complex moment orientations due to the underlying orbital interaction [7]. RXS at the Dy L_3 edge has been used to elucidate Dy dipole and quadrupole motifs [6, 8]. A dipole transition (E1) occurs between Dy $2p$ and $5d$ shells and a quadrupole transition (E2) between Dy $2p$ and $4f$ shells. The first and dominant process probes the quadrupolar order of the $5d$ states and the latter transition probes the quadrupolar order of the $4f$ states. The quadrupolar origin of the reflection has been confirmed by azimuthal scans (rotation around the Bragg wave vector).

Ground state wave functions of the Dy $4f$ shell have been proposed based on the observed absence of E2 intensity at the $(00\frac{5}{2})$ charge forbidden reflection which implied cancellation of quadrupole (rank 2) and hexadecapole (rank 4) contributions [9]. These wave-functions are consistent with a recent inelastic neutron scattering study where the orbital fluctuation timescale has been determined [10]. An alternative explanation for the RXS data suggest that the hexadecapole moment is zero and the overlap between the E1 and E2 resonances cancels the E2 intensity [11]. However, this analysis is not sound [12]. SXRS at the Dy $M_{4,5}$ edges accesses the $4f$ shell directly with the E1 transition, *without* the complication of overlapping E1 and E2 resonances. Our results show that the Coulomb (intra-atomic quadrupole) interaction between the $3d$ and $4f$ shells is significant. The ordered quadrupole moment of the $4f$ shell in the intermediate state reshapes the observed $3d_{5/2}$ and $3d_{3/2}$ electron density and leads to a core hole splitting. It is shown that this phenomenon causes interference between

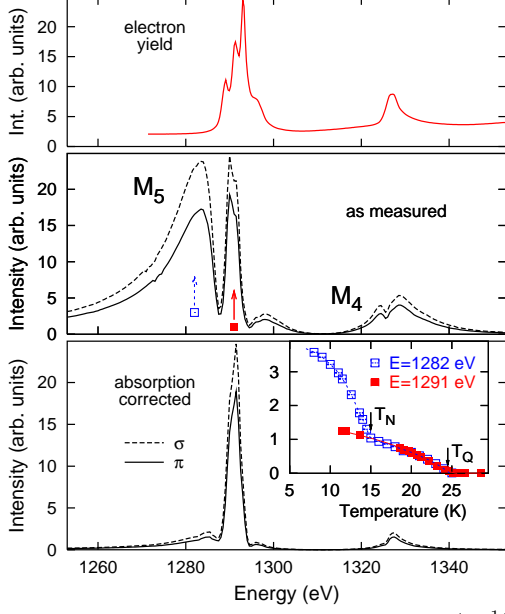


FIG. 1: Diffraction intensity of orbital ordering ($00\frac{1}{2}$) reflection in DyB_2C_2 taken with incident σ and π polarization at $T=18$ K (middle). Top graph shows the absorption recorded in electron yield and the bottom graph shows the diffracted intensity after correction for absorption. The inset shows the intensity as a function of temperature for $E=1282$ eV and 1291 eV.

different pathways of the scattering amplitude allowing the extraction of high-order multipole moments of the $4f$ shell that have rank 4 and rank 6 (hexacontatetrapole).

A DyB_2C_2 single crystal has been grown by Czochralski method using an arc-furnace with four electrodes and cut with (001) perpendicular to the sample surface. Subsequently, it was polished and aligned with 26° azimuthal angle. Zero degrees azimuth corresponds to alignment of the b axis in the scattering plane. The orbital ordering ($00\frac{1}{2}$) reflection has been recorded at the Dy $M_{4,5}$ edges of DyB_2C_2 at the RESOXS end-station of the SIM beam-line at the Swiss Light Source. The Dy $M_{4,5}$ absorption edges have been characterized with fluorescence yield (FY) and electron yield (EY) at RESOXS and the BL25SU beam line at SPring-8, respectively.

The energy profile of the charge forbidden ($00\frac{1}{2}$) reflection, together with x-ray absorption (XAS) data (EY), is shown in Fig. 1. Multiple features are observed with much larger energy spread than the multiplet structure of the XAS data, in contrast with the single oscillator recorded at the Dy L_3 edge [9]. A similar energy profile has been reported for the M_5 edge of Ho at the magnetic $(0,0,\tau)$ reflection but the central sharp feature (solid symbol in Fig. 1) is absent [13]. The authors argue that the large photo-absorption causes this ‘gap’ at the M_5 edge because strong absorption is inherent to soft x-ray scattering. To characterize the width of the scattering $\theta/2\theta$ -scans have been recorded for the ($00\frac{1}{2}$) reflection at each energy. Comparison with FY and EY data shows part of the width is due to the limited penetration depth. Sub-

sequently, the integrated intensity has been corrected for absorption as shown in the bottom panel of Fig. 1. Absorption effects hugely reduce the intensity of the central feature but cannot account for the multiple features in the energy dependent intensity. The different character of those structures becomes even more apparent from the temperature dependence of the scattered intensity. The AFM transition is witnessed at 15 K as a gradual increase in intensity at 1282 eV, however this increase is absent at 1291 eV (see inset of Fig. 1). This cannot be caused by absorption effects on a single oscillator resonance. It appears that the scattered intensity at 1291 eV is sensitive to the orbital order only and its gradual increase below T_N shows that there is no lock-in of the orbitals as proposed from neutron diffraction and symmetry analysis [14].

The structure in the energy profile is similar for σ and π polarization of the incident x-rays and independent of the sample temperature in the AFQ phase. Azimuthal angles of 56° and 86° give the same spectral shape but show different overall intensity as expected from the azimuthal angle dependence of a quadrupole. This illustrates merely one atomic tensor is active in the scattering process. We propose that this particular shape of the energy dependence of the ($00\frac{1}{2}$) reflection is caused by the splitting of the $3d$ core states which results in multiple interfering resonators and consequently adds structure to the energy profile. Previously a core hole splitting caused by the intra-atomic magnetic interaction between $5f$ and $3d$ was used to describe the unusual double Lorentzian energy profile at the M_4 resonance in NpO_2 [15]. There is no ordered magnetism in the AFQ phase and we introduce the intra-atomic *quadrupolar* interaction to partially lift the core hole degeneracy. The energy splitting is determined by the strength of the intra-atomic interaction and we show that the relative amplitudes are determined by the $4f$ wave function. Thus, the spectral shape is constant in the AFQ phase. Note that the diffracted intensity is caused by the bulk order and subject to critical fluctuations while the energy splitting is due to the local orbital moment of the $4f$ shell and independent of its orientation. We will first encapsulate the resonant diffraction theory specific to our problem and introduce the intra-atomic quadrupole interaction to portray the observed energy dependence.

The scattered photon intensity $d\sigma/d\Omega$ is proportional to the squared modulus of the amplitude f [16]

$$f = \sum_{K,Q} (2K+1)^{\frac{1}{2}} X_{-Q}^K \sum_q D_{Qq}^K(\alpha, \beta, \gamma) F_q^K, \quad (1)$$

which is described as a product of spherical tensors with rank K . F_q^K with $-K \leq q \leq K$ describes the electronic response of the sample. X_{-Q}^K with $-K \leq Q \leq K$ describes the geometry of the experimental set-up and polarization direction of the incident and reflected x-rays.

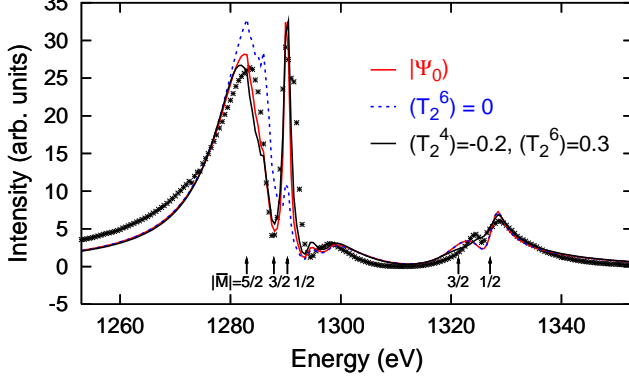


FIG. 2: Observed energy profile (crosses) compared to fits of the theory including absorption correction with a) wave-function taken from Ref. [9] (red), b) $\langle T_2^6 \rangle$ set to zero (dotted blue), and c) $\langle T_2^x \rangle$ as free parameter (black). $\langle T_2^2 \rangle$ is normalized to 1, $\langle T_2^4 \rangle = -0.2$, $\langle T_2^6 \rangle = +0.3$, $\Gamma_{\frac{5}{2}, \pm \frac{1}{2}} = 0.8$ eV, $\Gamma_{\frac{5}{2}, \pm \frac{3}{2}} = 2.7$ eV, $\Gamma_{\frac{5}{2}, \pm \frac{5}{2}} = 5.3$ eV, $\Gamma_{\frac{3}{2}, \pm \frac{1}{2}} = 1.9$ eV and $\Gamma_{\frac{3}{2}, \pm \frac{3}{2}} = 5.4$ eV.

Lastly, $D_{Qq}^K(\alpha, \beta, \gamma)$ rotates F_q^K onto the coordinates of the experimental reference frame used for X_{-Q}^K with Euler angles α, β, γ . The Dy site symmetry of $2/m$ gives $q = \pm 2$ and $K = 2$ due to the absence of charge ($K = 0$) and time-odd (magnetic) ($K = 1$) order at $(00\frac{1}{2})$ in the AFQ phase.

F_q^K describes the atomic resonant process which is commonly represented by a harmonic oscillator. In our particular case F_q^K is a sum of several oscillators at the E1 resonance created by the splitting of the core state. The amplitude $A_q^K(\bar{J}, \bar{M})$ of each oscillator is labeled by the total angular momentum $\bar{J} = \frac{3}{2}, \frac{5}{2}$ and magnetic quantum number \bar{M} of the core hole.

$$F_q^K \propto \sum_{\bar{J}, \bar{M}} \frac{r_{\bar{J}} A_q^K(\bar{J}, \bar{M})}{E - \Delta_{\bar{J}} - \epsilon(\bar{J}, \bar{M}) + i\Gamma_{\bar{J}, \bar{M}}}. \quad (2)$$

Here, E is the photon energy, $\Delta_{\bar{J}}$ is the difference in energy between the degenerate $3d_{\bar{J}}$ shell and the $4f$ empty states and $\Gamma_{\bar{J}, \bar{M}}$ the lifetime of the intermediate state. $\epsilon(\bar{J}, \bar{M}) = [3\bar{M}^2 - \bar{J}(\bar{J} + 1)]Q_{\bar{J}}$ is the energy shift of the $3d$ core levels due to the intra-atomic quadrupole interaction $Q_{\bar{J}}$, similar as in Mössbauer spectroscopy. $Q_{\bar{J}}$ is a product of the $3d$ quadrupole moment and the f -electron electric field gradient experienced by the $3d$ electrons with $Q_{\pm \frac{3}{2}}/Q_{\pm \frac{5}{2}} = 7/3$.

The amplitudes interfere and the branching ratio between the two edges is defined as a real mixing parameter $r_{\bar{J}}$. $A_q^K(\bar{J}, \bar{M})$ is constructed from the structure factor of the chemical unit cell Ψ_q^x

$$A_q^K(\bar{J}, \bar{M}) = (-1)^{\bar{J}-\bar{M}} \sum_r (2r+1) \begin{pmatrix} \bar{J} & r & \bar{J} \\ -\bar{M} & 0 & \bar{M} \end{pmatrix} \times \sum_x \begin{pmatrix} K & r & x \\ -q & 0 & q \end{pmatrix} R^K(r, x) \Psi_q^x, \quad (3)$$

where $R^K(r, x)$ are reduced matrix elements, $r = 0, 1, \dots, 2\bar{J}$, $x = |K-r|, \dots, |K+r|$ and $q+x$ and $r+x$ equal an even integer. The Dy site symmetry, $2/m$, dictates that $A_2^2 = -A_{-2}^2$ and $\Psi_q^x = \langle T_q^x \rangle - \langle T_{-q}^x \rangle$ where $\langle T_q^x \rangle = \langle \Psi_0 | T_q^x | \Psi_0 \rangle$, T_q^x is the atomic spherical tensor of the Dy $4f$ shell and $|\Psi_0\rangle$ its ground state wave function. It follows that $A_q^K(\frac{5}{2}, \bar{M})$ contains the hexadecapole moment $\langle T_2^4 \rangle$ and hexacontatetrapole moment $\langle T_2^6 \rangle$ in addition to the quadrupole moment $\langle T_2^2 \rangle$. In case $\epsilon(\bar{J}, \bar{M}) = 0$ the terms proportional to $\langle T_2^4 \rangle$ and $\langle T_2^6 \rangle$ cancel and $A_q^K(\bar{J})$ is proportional to $\langle T_2^2 \rangle$ as usual.

Let us here summarize the consequences of this analysis of the scattering. The overall intensity is well represented by scattering from the quadrupole $\langle T_2^2 \rangle$ of the $4f$ shell and reflects the same azimuthal angle dependence as the quantity observed in the dipole transition at the L_3 edge [9]. The dependence on the higher $4f$ multipoles arises from the splitting of the core hole states, which results in the \bar{M} dependence of the amplitudes of the different harmonic oscillators (Eq. 2). Correspondingly, these amplitudes are influenced by higher $4f$ multipoles as shown in Eq. 3 (Wigner-Eckart theorem). Therefore, the core hole splitting allows, for the first time, to measure the ordered hexacontatetrapole moment of an electronic shell in solid state physics. Note, that this is not in contradiction with the fact that the integrated intensity of a dipole (E1) transition is sensitive to tensors up to rank 2 (quadrupole), while a quadrupole (E2) transition is sensitive to tensors up to rank 4 (hexadecapole).

Figure 2 shows the measured energy dependence compared to the above theory including absorption effect. This model describes the data well. $\Delta_{\bar{J}}$ typically depicts the onset of an absorption edge and $r_{\frac{3}{2}}$ is calculated by Ref. [17] at 0.22 which is in excellent agreement with our SXRS data. $Q_{\frac{5}{2}} = -0.4$ eV and the resonance positions are indicated in Fig. 2. The linewidth increases progressively from 0.8 eV for $\bar{M} = \pm \frac{1}{2}$ to 5.3 eV for $\bar{M} = \pm \frac{5}{2}$. $|A_q^K(\frac{5}{2}, \pm \frac{3}{2})|$ is relatively small. Variations in $\langle T_2^x \rangle$ can be partially compensated by the line widths to yield a similar result. The best fit gives $\langle T_2^4 \rangle = -0.2$ and $\langle T_2^6 \rangle = 0.3$ while the $4f$ ground state wavefunction taken from Ref. [9] gives $\langle T_2^4 \rangle = -0.57$ and $\langle T_2^6 \rangle = 0.36$ and describes the data also well. The corresponding fits as well as the effect of setting $\langle T_2^6 \rangle$ to zero are shown in Fig. 2 [18]. The temperature dependence observed at 1282 eV and 1291 eV supports our analysis since the resonant cross section contains additional time odd terms due to the magnetic order below T_N . These terms may add at $\epsilon(\frac{5}{2}, \pm \frac{5}{2})$ while they cancel at $\epsilon(\frac{5}{2}, \pm \frac{1}{2})$.

The Dy $4f$ charge density obtained from the best fit is illustrated in Fig. 3. It supports a 90° zig zag alignment along c as demonstrated by its protrusions at top and bottom. In the basal plane a 90° zig zag alignment along $[110]$ is preferred so that the concave part points toward the convex part of its nearest neighbor. Yet, the absence of lock-in of the orbitals confirm that the orbital motif

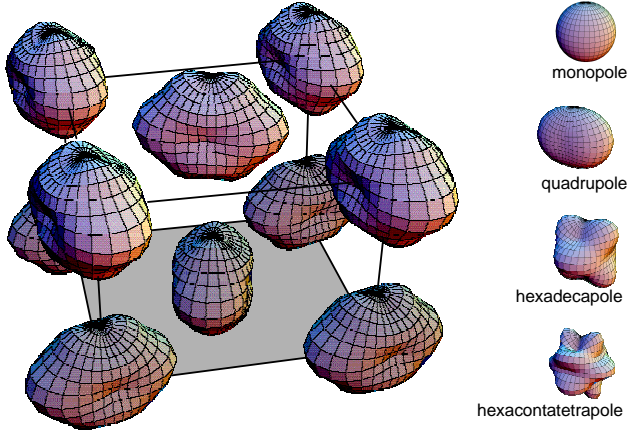


FIG. 3: Dy charge density and multipole motif in the AFQ phase of DyB_2C_2 . The basal plane is indicated in gray. Note the 90° zig zag alignment of the Dy orbitals along c and the canted zig zag alignment along $[110]$. A spherical charge density has been subtracted to emphasize the asphericity.

in the AFQ phase is similar to that in the AFQ+AFM phase and the Dy charge densities are canted away from $[110]$ [7]. Such an AFQ structure logically emerges when the pairwise movement of B and C ions is in competition with the multipolar interaction and promotes parallel alignment of the orbitals along $[110]$ [19]. In contrast, the 90° zig zag alignment along c is supported by both mechanisms. This is consistent with a recent study of $(\text{Dy,Y})\text{B}_2\text{C}_2$ where quasi one dimensional AFQ along the c axis has been reported [20].

We should add that our analysis in terms of core valence interaction is consistent with the multiplet structure interpretation. In the M_5 and M_4 absorption the multiplet structure is ~ 10 eV and ~ 5 eV wide, respectively, which is mainly due to the strong $3d-4f$ and $4f-4f$ Coulomb and exchange interactions [17]. The $3d_{5/2}^9 4f^{10}$ and $3d_{3/2}^9 4f^{10}$ final state multiplets contain 6006 and 4004 levels with an average lifetime width of 0.27 eV and 0.55 eV, respectively. The strong electron correlation leads to non-diagonal matrix elements in the quantum numbers $\bar{L}\bar{S}\bar{J}$ of the core hole. The levels of the same \bar{M} connected by these non-diagonal elements excite partly coherent. This makes it difficult to separate the core hole states. In the free ion we do not expect an energy shift for distributions of different $|\bar{M}|$. This was confirmed for the x-ray absorption spectrum with Cowan's atomic Hartree-Fock code, where we found roughly an equally broad multiplet when switching off the quadrupole component of the orbital contribution of the core-valence interaction. This suggests that any energy shifts in the $|\bar{M}|$ distributions will be due to multipolar ordering of the $4f$ states.

In this theoretical framework the core hole state is uncoupled from the $4f^{n+1}$ state and the effect of the $4f$

multiplet structure is indirectly taken into account by the effective widths of the \bar{M} distributions, which exceed the intrinsic life time width and describes the data surprisingly well.

In conclusion, the Dy $4f$ hexadecapole and hexacontatetrapole moments in DyB_2C_2 have been measured with SXRS and their magnitudes are determined at -20% and $+30\%$ of the quadrupole moment, respectively. The orbital order remains unaffected by magnetic order below T_N and no lock-in of the orbitals takes place, in contrast to CeB_6 . The structural transition and multipolar interactions cooperate along the c axis while they compete along $[110]$. These findings amply demonstrate a new extension of the resonant x-ray Bragg diffraction method for the observation of high-order electronic multipole motifs. Of particular interest are materials in which higher order multipoles are believed to be of importance, such as CeB_6 , URu_2Si_2 as well as the RB_2C_2 and skutterudite families.

We thank O. Zaharko for valuable discussion. This work was supported by the Swiss National Science Foundation and performed at the SLS of the Paul Scherrer Institute, Villigen PSI, Switzerland.

-
- [1] H. M. Al-Khateeb, B. G. Birdsey, and T. J. Gay, Phys. Rev. Lett. **85**, 4040 (2000), Phys. Rev. A **71**, 032707 (2005).
 - [2] V. P. Plakhty *et al.*, Phys. Rev. B **71**, 100407(R) (2005).
 - [3] K. Kubo and T. Hotta, Phys. Rev. B **71**, 140404(R) (2005).
 - [4] A. Kiss and P. Fazekas, Phys. Rev. B **71**, 054415 (2005).
 - [5] H. Adachi *et al.*, Phys. Rev. Lett. **89**, 206401 (2002).
 - [6] Y. Tanaka *et al.*, J. Phys.: Condens. Matter **11**, L505 (1999).
 - [7] H. Yamauchi *et al.*, J. Phys. Soc. Jpn **68**, 2057 (1999).
 - [8] K. Hirota *et al.*, N. Oumi, Phys. Rev. Lett. **84**, 2706 (2000).
 - [9] Y. Tanaka *et al.*, *et al.*, Phys. Rev. B **69**, 024417 (2004).
 - [10] U. Staub *et al.*, Phys. Rev. Lett. **94**, 036408 (2005).
 - [11] T. Matsumura *et al.*, Phys. Rev. B **71**, 012405 (2005).
 - [12] The mixing parameter of E1 and E2 processes is fixed at unity in the analysis but this is not a priori justified.
 - [13] P. Spencer *et al.*, J. Phys.: Condens. Matter **17**, 1725 (2005).
 - [14] O. Zaharko *et al.*, Phys. Rev. B **69**, 224417 (2004).
 - [15] S. W. Lovesey *et al.*, J. Phys.: Condens. Matter **15**, 4511 (2003).
 - [16] S. W. Lovesey *et al.*, Phys. Rep. **411**, 233 (2005).
 - [17] B. T. Thole *et al.*, Phys. Rev. B **32**, 5107 (1985).
 - [18] Note that the reduced matrix elements are contained in Eq. (3) while in Ref. [9] they are included in $\langle T_2^x \rangle$.
 - [19] See Fig. 4b of ref. [14] for specific movement of B and C.
 - [20] K. Indoh *et al.*, J. Phys. Soc. Jpn **73**, 1554 (2004).